PBI-BFS-MaOA: A Many-Objective Evolutionary Algorithm with PBI-Based Boundary-Front Selection

ARTICLE HISTORY
Received 8 March 2026
Accepted 26 May 2026
Published 7 July 2026

Thiago Santos
Federal University of Ouro Preto (UFOP)
Associate Professor
Ph.D. in Mathematics
Brazil
santostf@ufop.edu.br
ORCID: 0000-0002-2435-2786

Sebastião Xavier
Federal University of Ouro Preto (UFOP)
Associate Professor
Ph.D. in Mathematics
Brazil
semarx@ufop.edu.br
ORCID: 0009-0004-2765-0764

ISSN:1390-9266 e-ISSN:1390-9134 LAJC 2026

PBI-BFS-MaOA: A Many-Objective Evolutionary Algorithm with PBI-Based Boundary-Front Selection

Thiago Santos
Federal University of Ouro Preto (UFOP)
Associate Professor
Ph.D. in Mathematics
Brazil
santostf@ufop.edu.br

Sebastião Xavier
Federal University of Ouro Preto (UFOP)
Associate Professor
Ph.D. in Mathematics
Brazil
semarx@ufop.edu.br

***Abstract*—Reference-guided many-objective evolutionary algorithms often lose selection pressure when Pareto dominance becomes scarce and the final accepted front must be truncated. We propose PBI-BFS-MaOA, a many-objective evolutionary algorithm that preserves Pareto ranking for feasible solutions and modifies only the survival decision on the boundary front. The method combines cumulative ideal–nadir normalization, penalty-based boundary intersection association, active-niche filtering, and occupancy-aware survivor insertion. These operations are activated where convergence and directional coverage must be decided simultaneously. We evaluate the algorithm on DTLZ1–DTLZ4 and WFG1–WFG4 with $M \in \{5, 8, 10\}$ objectives, using the averaged Hausdorff distance Δ_p, Wilcoxon signed-rank tests, Friedman rank analysis, and runtime measurements. PBI-BFS-MaOA obtains the best mean Δ_p in 13 of 24 benchmark instances, with its strongest gains on high-dimensional DTLZ cases and degenerate WFG3 instances, while its runtime remains between NSGA-III and CMOEA-CD.**

***Keywords*—many-objective optimization, environmental selection, reference directions, penalty-based boundary intersection**

I. Introduction

Many-objective optimization is difficult not only because more criteria must be evaluated, but because Pareto dominance rapidly loses its ability to separate candidate solutions. Li et al. [1] identify this loss of discrimination as a central obstacle once the number of objectives moves beyond the classical two- or three-objective setting. Santos and Takahashi [2] give a formal account of the same phenomenon: as objective dimensionality increases, the probability that one candidate dominates another decreases sharply. The population then accumulates mutually non-dominated solutions, and environmental selection must choose among candidates that the initial dominance relation no longer orders with enough contrast.

This loss of contrast changes the role of survival selection. After the clearly superior fronts have been accepted, the remaining population slots are often disputed by an overflowing boundary front. At that point, the algorithm must preserve convergence while still maintaining directional coverage. The problem is geometric as much as statistical. In high-dimensional objective spaces, local density is harder to estimate, front shapes are harder to interpret, and unsupported reference directions may receive attention simply because the selection rule lacks a sharper local signal. Pal et al. [3] discuss a related difficulty from the perspective of objective reduction: deciding which information remains relevant becomes itself a nontrivial design problem.

Several algorithmic families address this pressure from different angles. Decomposition methods organize search through scalar subproblems, as in MOEA/D [4], and dominance-decomposition hybrids such as MOEA/DD [5] show that Pareto ordering and directional structure can coexist in the same survival mechanism. Reference-guided algorithms follow a related geometric logic. NSGA-III [6], θ-DEA [7], and RVEA [8] all use reference information to recover discrimination when non-dominated sets become too large. Their shared premise is clear: many-objective selection needs more than front rank.

Directional guidance, however, is not neutral. Ishibuchi et al. [9] show that decomposition-based performance is strongly affected by Pareto-front shape. A reference structure that works well on a regular front may become less reliable on disconnected, biased, or degenerate geometries. Qiu et al. [10], Liu et al. [11], Li et al. [12], and Wang et al. [13] respond to this issue by adapting reference structures or strengthening dominance with reference-vector information. These contributions suggest that survival quality depends not only on having directions, but on deciding which directions are actually supported by the current population.

The present work focuses on that decision at a narrower location: the boundary front. We do not replace Pareto ranking, redefine dominance globally, or introduce a multiarchive search architecture. Instead, PBI-BFS-MaOA preserves the usual Pareto scaffold for feasible solutions and intervenes only when the first overflowing front must be truncated. The proposed survival rule combines cumulative ideal–nadir normalization, penalty-based boundary intersection association, active-niche filtering, and occupancy-aware insertion. The aim is to use geometric information exactly where ordinary front ordering becomes underdetermined.

This local view has practical value in technological decision problems where many objectives must be balanced under a limited evaluation budget. Engineering design, energy dispatch, logistics planning, portfolio allocation, scheduling, and resource management often require simultaneous trade-

ISSN:1390-9266 e-ISSN:1390-9134 LAJC 2026
DOI: https://doi.org/10.33333/lajc.vol13n2.04

offs among cost, reliability, risk, environmental impact, and service quality. In such settings, wasting evaluations on poorly supported directions can delay the discovery of usable compromises. A boundary-front rule that protects the global Pareto order while improving the last survival decision is therefore relevant beyond benchmark optimization.

We evaluate the proposed intervention on DTLZ and WFG benchmark families with $M \in \{5, 8, 10\}$ objectives in the PymooLab environment [14]. Performance is measured with the averaged Hausdorff distance Δ_p, Wilcoxon signed-rank tests, Friedman rank analysis, and runtime measurements. NSGA-III and CMOEA-CD serve as structurally distinct baselines: the first is the canonical reference-guided Pareto method, and the second is a recent archive-cooperation approach. Section II places the proposal in the literature, Section III defines the survival rule, Section IV reports the numerical protocol and results, and Section V concludes the paper.

II. Related Work

The many-objective literature can be organized around a common design question: once Pareto dominance no longer separates most candidates, where should additional discrimination enter the evolutionary pipeline? Some methods modify the global search decomposition, others adapt the reference structure, and still others revise the dominance relation. The present work belongs to the environmental-selection line, but it is useful to position it against these alternatives [1].

Decomposition-based methods were among the earliest scalable responses. Zhang and Li [4] distributed the search across scalar subproblems, thereby reducing reliance on global pairwise dominance. Li et al. [5] later combined dominance and decomposition in MOEA/DD. This line of work established a key principle for many-objective search: front rank and directional scalarization can operate at different resolutions. Pareto order can maintain the broad convergence scaffold, while a directional mechanism can resolve local competition among candidates that are otherwise difficult to separate.

Reference-guided methods express the same principle in geometric form. Deb and Jain [6] used reference points to guide environmental selection in NSGA-III, which remains the most direct baseline for a modified reference-based survival stage. Yuan et al. [7] introduced angular information through θ-DEA, and Cheng et al. [8] built RVEA around reference-vector-guided survival. These algorithms differ in implementation, but they share a central conclusion: once non-dominated sets become too large, directional information is needed to make survival decisions operational.

That conclusion must be qualified. Ishibuchi et al. [9] show that decomposition-based algorithms are highly sensitive to Pareto-front shape. A fixed reference structure may be effective on regular fronts and less reliable on disconnected, biased, or degenerate fronts. Qiu et al. [10] improved objective-space decomposition under this concern, while Liu et al. [11], Li et al. [12], and Wang et al. [13] introduced self-guided, redistributed, or reference-vector-based dominance mechanisms. The common lesson is that the reference structure should not be treated as automatically valid everywhere in the objective space.

A second line preserves Pareto semantics while weakening or extending its strict form. Zhu et al. [15] generalized Pareto optimality for many-objective search. Tian et al. [16] strengthened dominance by combining convergence and diversity information, and Zhu et al. [17], [18] later developed generalized or relaxed dominance as a broader design framework. These methods show that dominance can be repaired, but they often act globally even though the strongest ambiguity may occur at a specific survival stage.

Environmental-selection studies make that local ambiguity explicit. Cheng et al. [19] argued that mating and environmental selection should be designed jointly, because the quality of selected parents is inseparable from the survival pressure they face. Sharma and Shukla [20] studied line-prioritized normalization and survivor choice, Myszkowski and Laszczyk [21] investigated diversity-based selection under constraints, and Liu et al. [22] treated environmental selection through clustering. These contributions differ in mechanics, but they agree on a practical point: the final accepted front is not a bookkeeping remainder. It is often where convergence and spread are either preserved or lost.

CMOEA-CD [23] provides a recent contrast. Instead of modifying one stage of selection, it uses three collaborative archives: a forward-exploration archive, a diversity-enhancement archive, and a feasibility-exploitation archive. This architecture separates exploration, diversity recovery, and feasible-solution intensification across different population-management channels. It is broader than the design studied here, and for that reason it is a useful comparator. Our question is more restricted: can a focused intervention in the boundary front recover selection pressure without replacing the surrounding evolutionary framework?

PBI-BFS-MaOA is therefore positioned between reference-guided selection and environmental-selection refinement. It keeps the Pareto-front order intact, associates only the critical front with normalized PBI directions, filters directions that lack support from the leading front when the front coverage is clearly sparse, and inserts survivors with an occupancy-aware rule. The contribution is intentionally local. Its value is not that it redesigns the entire many-objective algorithm, but that it targets the point at which the standard reference-guided survival rule becomes least decisive.

III. Proposed Method

The proposed method is a generational many-objective evolutionary algorithm whose main contribution lies in environmental selection rather than reproduction. Sampling, mating, and variation follow a classical evolutionary backbone. The restricted question is whether survival selection can recover discrimination inside the boundary front without discarding the global Pareto scaffold. To do so, the method retains front-based ordering where the population already provides a clear rank structure and intervenes only when the first overflowing front must be trimmed. The implementation then applies cumulative ideal–nadir normalization, PBI-based association, active-niche filtering, and occupancy-aware insertion. The method is therefore a survival-stage refinement within the standard evolutionary loop, focused on the point where dominance contrast is weakest in practice.

ISSN:1390-9266 e-ISSN:1390-9134 LAJC 2026
DOI: https://doi.org/10.33333/lajc.vol13n2.04

Algorithm 1 Framework of the implemented PBI-BFS-MaOA

Input: population size N, reference directions $\mathcal{W}$, penalty parameter θ
Sample and evaluate the initial population $\mathcal{S}_0$
Initialize $\mathbf{z}^{\min}$ and $\mathbf{z}^{\max}$ from $\mathcal{S}_0$
Apply environmental selection to obtain $\mathcal{S}_0$ and its tournament fitness
while the stopping criterion is not met **do**
  Select parents by tournament using constraint violation and current fitness
  Generate offspring $\mathcal{Q}_t$ with a standard genetic variation operator
  Form the merged population $\mathcal{P}_t = \mathcal{S}_t \cup \mathcal{Q}_t$
  Update $\mathbf{z}^{\min}$ and $\mathbf{z}^{\max}$ from $\mathcal{P}_t$
  Apply environmental selection on $\mathcal{P}_t$
  Obtain the next population $\mathcal{S}_{t+1}$ and the updated tournament fitness
end while
Extract the current approximation set by filtering the population for feasible nondominated solutions

A. Framework of the Implemented Method

Let $\mathcal{S}_t$ denote the population at generation t, with $|\mathcal{S}_t| = N$, and let $\mathcal{W} = \{\mathbf{w}_1, \ldots, \mathbf{w}_K\}$ be the externally supplied set of reference directions. The process begins by sampling and evaluating an initial population, from which cumulative ideal and nadir estimates are initialized. Each generation then performs tournament-based parent selection, offspring generation by a standard variation operator, parent–offspring merging, and one environmental-selection call that returns both the survivors and the rank-based fitness values reused in the next tournament selection. Algorithm 1 summarizes the implemented architecture, and Fig. 1 presents the same process from the viewpoint of the survival decision.

The boundary-front rule is active from the first environmental-selection call onward, rather than being introduced as a late-stage correction. This matters because many-objective runs may produce large non-dominated subsets well before the final generations. The method is therefore directed at the $M > 3$ regime, where the last accepted front can dominate the survival outcome. The selection path moves through feasibility filtering, Pareto-front insertion, critical-front association, active-niche checking, and occupancy-aware insertion.

B. PBI-Based Boundary-Front Selection

Given the merged population $\mathcal{P}_t$, aggregated constraint violation is computed for each candidate $x_i \in \mathcal{P}_t$ as

$$\mathrm{CV}(x_i) = \sum_j \max\{0, g_j(x_i)\}. \tag{1}$$

This value induces the feasible subset

$$\mathcal{P}_t^f = \{x_i \in \mathcal{P}_t : \mathrm{CV}(x_i) = 0\}. \tag{2}$$

If $|\mathcal{P}_t^f| < N$, all feasible solutions are retained and the remaining slots are filled by the least infeasible candidates ranked by increasing CV. This branch is part of the implemented survival routine, although the numerical analysis in this paper uses unconstrained benchmark families. Its role is to establish a clear priority order: feasibility is handled first when feasible points are scarce, and the directional boundary-front rule is invoked only when enough feasible candidates exist for truncation to become the dominant issue.

When $|\mathcal{P}_t^f| \geq N$, selection proceeds on the feasible subset. The algorithm performs non-dominated sorting on the original objective vectors of $\mathcal{P}_t^f$ and obtains ordered fronts $\mathcal{F}_1, \mathcal{F}_2, \ldots$. Complete fronts are copied into the next population until the first overflowing front $\mathcal{F}_\ell$ is reached. Thus, the global convergence scaffold remains Pareto-ordered. The directional rule does not reshuffle clearly superior fronts; it acts only where Pareto ranking no longer determines the remaining survivor set.

The candidates in the critical front are then evaluated in normalized objective space. Let $\mathbf{z}_t^{\min}$ and $\mathbf{z}_t^{\max}$ denote the cumulative ideal and nadir estimates updated across generations. For an objective vector $\mathbf{f}_i$, the normalized vector is

$$\tilde{\mathbf{f}}_i = \frac{\mathbf{f}_i - \mathbf{z}^{\min}}{\max(\mathbf{z}^{\max} - \mathbf{z}^{\min}, \epsilon)}, \tag{3}$$

where ϵ is a componentwise safeguard against null spans. Each reference direction is normalized to unit length, and for every candidate–direction pair the algorithm computes

$$d_1(i,k) = \tilde{\mathbf{f}}_i^\top \mathbf{w}_k, \qquad d_2(i,k) = \sqrt{\|\tilde{\mathbf{f}}_i\|_2^2 - d_1(i,k)^2}. \tag{4}$$

The corresponding penalty-based boundary-intersection score is

$$\mathrm{PBI}(i,k) = d_1(i,k) + \theta_M d_2(i,k), \tag{5}$$

where

$$\theta_M = \begin{cases} \theta, & M \leq 3, \\ \theta\sqrt{M/3}, & M > 3. \end{cases} \tag{6}$$

Cumulative ideal–nadir normalization keeps directional comparisons stable across generations instead of allowing transient objective spans to dominate the association step. The PBI score separates an axial component d_1 from an orthogonal component d_2, so each candidate is evaluated by both progress along a direction and deviation from that direction. The scaling in (6) increases the orthogonal penalty as M grows, which is consistent with the stronger ambiguity observed in higher-dimensional objective spaces. The associated niche of x_i is then

$$k^\star(i) = \arg\min_k \mathrm{PBI}(i,k). \tag{7}$$

This association does not treat each direction as an independent scalar subproblem in the MOEA/D sense [4]. It provides a local geometric view only for candidates that have already passed Pareto-front screening.

C. Active-Niche Filtering and Occupancy-Aware Insertion

Once the complete fronts have been accepted, let $\mathcal{A}_t$ denote survivors already inserted before truncating the boundary front $\mathcal{F}_\ell$. Current occupancy is calculated for every niche k:

$$c_k = |\{x_i \in \mathcal{A}_t : k^\star(i) = k\}|. \tag{8}$$

ISSN:1390-9266 e-ISSN:1390-9134 LAJC 2026
DOI: https://doi.org/10.33333/lajc.vol13n2.04

LATIN-AMERICAN JOURNAL OF COMPUTING (LAJC), Vol XIII, Issue 2, July 2026

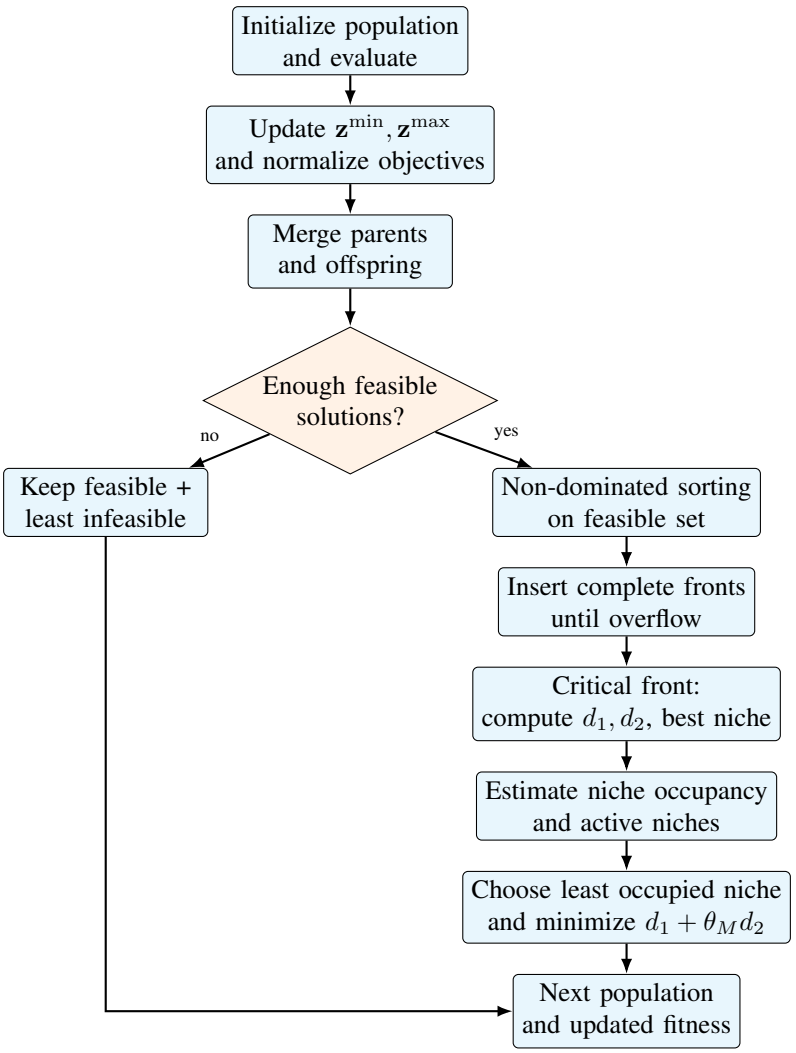

Fig. 1: Conceptual flow of the implemented PBI-BFS-MaOA survival mechanism

This occupancy count drives the boundary-front insertion rule. Additionally, the niche set that the first Pareto front activates is extracted in the algorithm:

$$\Omega_t = \{k^\star(i) : x_i \in \mathcal{F}_1\}. \tag{9}$$

If $|\Omega_t| < 0.8K$, the implementation treats the current leading front as insufficiently spread over the reference set. In that case, when the intersection is nonempty, only niches represented by $\mathcal{F}_\ell$ and active in Ω_t are admissible. Otherwise, all boundary-front niches remain admissible. The first front therefore acts as the support signal: if the best feasible solutions occupy only a restricted subset of directions, the algorithm avoids spending survivor slots on directions that the current population does not substantively support.

The $0.8K$ threshold is a conservative coverage gate rather than a tuned benchmark-specific parameter. It activates filtering only when at least 20% of the reference directions are unsupported by the leading front. This choice separates broadly covered fronts from fronts with visibly sparse directional support while avoiding the overly aggressive behavior that would arise from filtering whenever a small number of directions is missing. The value is also easy to interpret operationally: active-niche filtering is used only when the first front no longer represents most of the reference scaffold.

The last rule for insertion acts one survivor at a time. Every step identifies the least-occupied admissible niches, breaks ties randomly, and selects one niche. Let $\mathcal{C}_k \subseteq \mathcal{F}_\ell$ denote the candidates now assigned to the chosen niche k. The selected candidate is

$$x^\star = \arg\min_{x_i \in \mathcal{C}_k} \left(d_1(i, k^\star(i)) + \theta_M d_2(i, k^\star(i))\right). \tag{10}$$

This rule couples two pressures that in many-objective survival are often in tension. Poor niche occupancy allows for angular spread throughout the reference structure, and the within-niche PBI minimization favors candidates with better local convergence relative to the selected direction. The design is deliberately local. It does not change the ranking relation for the entire population, nor does it try to find a new global density model. It resolves the specific ambiguity created by the critical front after the better-ranked fronts have already been accepted.

After insertion, survivors receive rank-based fitness values according to their Pareto-front index. These values, together with constraint violation, are reused by tournament selection. Offspring generated by the variation operator are then merged back into the population, and the same survival rule is applied again. The empirical behavior reported in this paper should

ISSN:1390-9266 e-ISSN:1390-9134 LAJC 2026
DOI: https://doi.org/10.33333/lajc.vol13n2.04

therefore be read as the effect of a repeated boundary-front decision, not as a one-time tie-breaking operation.

The additional computational cost is concentrated in the critical-front association and insertion stage. Let $n_f = |\mathcal{P}_t^f|$ be the number of feasible candidates, $b = |\mathcal{F}_\ell|$ the size of the boundary front, K the number of reference directions, M the number of objectives, and r the number of remaining survivor slots. Non-dominated sorting over the feasible subset follows the usual front-ranking cost. The proposed modification adds $O(bKM)$ operations for normalized PBI association, $O(n_f + K)$ operations to compute current niche occupancy and active niches, and up to $O(r(b + K))$ operations for iterative occupancy-aware insertion under a direct implementation. Since $r \leq b$, the added survival-stage cost is bounded by $O(bKM + b^2 + bK + n_f)$. This is higher than the simplest NSGA-III niching pass, but it remains localized to the boundary front and is consistent with the observed runtime profile: slower than NSGA-III, yet substantially cheaper than the broader multiarchive management used by CMOEA-CD.

D. Design Highlights and Current Scope

The proposed approach has four active design choices. First, it keeps Pareto-front ordering as the global convergence scaffold and reserves directional scalarization for the moment at which that scaffold no longer determines the survivor set. Second, it uses cumulative ideal–nadir normalization to keep PBI association numerically stable across the run without excessive sensitivity to transient population spans. Third, it scales the orthogonal PBI penalty by $\sqrt{M/3}$ at $M > 3$, directly targeting the many-objective regime for which the method is designed. Fourth, it combines active-niche filtering and occupancy-aware insertion, making the boundary-front decision dependent on both local scalarization values and the current elite support of the reference structure.

These design choices also define the limits of the present claim. The constructor exposes the value σ_d, and the source file includes a helper for niche-penalty calculation, but in the current implementation that helper does not take part in the active survival path. The method is therefore not a fuzzy-dominance framework, a radial-repulsion mechanism, or a multiarchive strategy. The contribution, as evidenced in the code and by the benchmarks, is narrower and more specific: a Pareto-ordered many-objective evolutionary approach with normalized PBI-based boundary-front selection, conditional active-niche filtering, and occupancy-aware survivor insertion.

IV. Numerical Simulation and Analysis

A. Benchmark Test Problems

For the numerical study, we use two benchmark groups, namely DTLZ1–DTLZ4 [24] and WFG1–WFG4 [25], with objective counts $M \in \{5, 8, 10\}$. These settings place each experiment in the many-objective regime for which the proposed survival rule was developed. The benchmark families are deliberately complementary. DTLZ provides canonical and relatively interpretable front structures, while WFG introduces stronger distortions in shape, modality, deceptiveness, and degeneracy. Taken together, the two suites test whether the mechanism works only on regular fronts or also under geometries where reference-guided truncation is more difficult.

The DTLZ family isolates complementary sources of difficulty. DTLZ1 has a linear Pareto front with strong multimodality, making it useful for testing whether the boundary-front rule remains stable under competing local attractors. DTLZ2 has a smooth spherical front and provides a cleaner directional-coverage test. DTLZ3 retains the DTLZ2 geometry but adds severe multimodality, making it a difficult convergence test without changing the fundamental front shape. DTLZ4 biases the mapping toward extreme regions and is relevant for methods that depend on directional balance.

The WFG suite directs the evaluation toward more irregular geometries. WFG1 adopts bias and mixed shape transformations, while WFG2 generates disconnected and deceptive structures. WFG3 produces degenerate fronts, and WFG4 adds strong multimodality. WFG3 is particularly relevant because degeneracy is the scenario in which active-niche filtering should have its clearest effect.

We vary the number of objectives from 5 to 8 and 10 to test whether the local survival logic becomes more relevant as the selection stage grows more crowded.

B. Algorithms Comparison and Experimental Settings

The benchmark compares PBI-BFS-MaOA with two structurally relevant baselines: NSGA-III [6] and CMOEA-CD [23]. NSGA-III is the direct baseline because it combines Pareto fronts with reference directions and performs environmental selection through reference-guided niching. It is therefore the natural comparator for testing whether a new boundary-front rule improves a reference-guided survival protocol without changing the broader evolutionary paradigm.

CMOEA-CD is included for a different reason. Instead of relying on a single environmental-selection regime, it organizes a forward-exploration archive, a diversity-enhancement archive, and a feasibility-exploitation archive. Although CMOEA-CD was proposed for constrained multiobjective optimization, it remains informative here because it represents a recent and technically sophisticated alternative to single-stage survivor selection. The comparison therefore contrasts a local boundary-front intervention with a broader archive-cooperation design.

All algorithms are run in the PymooLab framework [14]. For every problem instance, the population size is fixed at 100, the maximum number of function evaluations is fixed at 50,000, and 30 independent runs are performed. The benchmark harness uses independent random seeds and records the indicator values and summary statistics used in the final performance evaluation.

NSGA-III and PBI-BFS-MaOA use the same reference-direction generation logic, which keeps the comparison focused on the survival operator rather than on different directional sets. For each instance, we report the mean and standard deviation of the performance indicator, the winning algorithm, the percentage gain of the winner over the closest comparator, and the pairwise Wilcoxon decision marker. This structure supports three readings: instance-wise comparison through the table, suite-wise comparison through Friedman

ISSN:1390-9266 e-ISSN:1390-9134 LAJC 2026
DOI: https://doi.org/10.33333/lajc.vol13n2.04

ranks, and computational-cost comparison through runtime statistics.

C. Experimental Results on Benchmark

The main performance indicator is Δ_p, the averaged Hausdorff distance between the approximation set returned by an algorithm and a reference Pareto front [26]. Let A denote the approximation set and let P^* denote the reference Pareto front. For a point u and a finite set S, define

$$d(u, S) = \min_{s \in S} \|u - s\|_2. \tag{11}$$

The p-averaged generational distance and inverted generational distance are written as

$$\mathrm{GD}_p(A, P^*) = \left(\frac{1}{|A|} \sum_{a \in A} d(a, P^*)^p \right)^{1/p}, \tag{12}$$

$$\mathrm{IGD}_p(A, P^*) = \left(\frac{1}{|P^*|} \sum_{p^* \in P^*} d(p^*, A)^p \right)^{1/p}. \tag{13}$$

Following Schütze et al. [26], the averaged Hausdorff distance is then

$$\Delta_p(A, P^*) = \max \left\{ \mathrm{GD}_p(A, P^*), \mathrm{IGD}_p(A, P^*) \right\}, \tag{14}$$

Lower Δ_p values indicate better performance because both convergence toward the reference front and spread along that front are penalized. The indicator is particularly relevant here because the proposed survival rule must negotiate convergence and diversity at the same stage.

A survival rule can reduce crowding while damaging local convergence, or improve convergence while collapsing directional coverage. Δ_p is sensitive to both failure modes and is therefore more stringent than a convergence-only indicator.

For each test instance, Table I reports the mean Δ_p value and sample standard deviation over 30 independent runs. Wilcoxon signed-rank tests are computed at significance level $\alpha = 0.05$ for pairwise comparisons, and Friedman tests are applied to compare average ranks across the DTLZ and WFG subsets.

The table is arranged as a single consolidated floating environment so that the full benchmark can be inspected at once. DTLZ and WFG are visually separated because the interpretation depends strongly on the distinction between canonical and distorted front geometries.

Table I shows that PBI-BFS-MaOA obtains the best mean Δ_p value in 13 of the 24 benchmark instances. NSGA-III is best in 7 cases, and CMOEA-CD is best in 4. The distribution of wins is more informative than the raw total. At $M = 5$, PBI-BFS-MaOA leads in only 2 of 8 cases, whereas at $M = 8$ and $M = 10$ it leads in $6/8$ and $5/8$ cases, respectively. This pattern agrees with the design motivation: as the number of objectives increases, the overflowing front becomes larger and less sharply separated under standard reference-guided selection, creating more room for a boundary-front intervention to help.

The DTLZ suite provides the clearest evidence in favor of the proposed approach. The Friedman test over the 12 DTLZ instances returns average ranks of 1.417 for PBI-BFS-MaOA, 1.833 for NSGA-III, and 2.750 for CMOEA-CD, with $\chi^2 = 11.167$ and $p = 3.76 \times 10^{-3}$. Pairwise Wilcoxon testing indicates a significant advantage of PBI-BFS-MaOA over CMOEA-CD ($p = 1.46 \times 10^{-3}$), while the difference from NSGA-III does not cross the 5% significance threshold ($p = 6.40 \times 10^{-2}$). Thus, on DTLZ, the proposed method clearly separates from CMOEA-CD and shows a repeated, although not statistically decisive, advantage over NSGA-III.

The strongest margins occur when multimodality and boundary-front pressure appear together. On DTLZ3 with $M = 10$, PBI-BFS-MaOA obtains $\Delta_p = 1.52$, compared with 21.9 for NSGA-III and 75.6 for CMOEA-CD. On DTLZ3 with $M = 8$, the corresponding values are 1.54, 14.3, and 19.8. For DTLZ1 with $M = 8$ and $M = 10$, the proposed method reaches 1.09×10^{-1} and 1.46×10^{-1}, compared with 2.00×10^{-1} and 4.71×10^{-1} for NSGA-III and much larger values for CMOEA-CD. These are precisely the cases in which many candidates can share the same front rank while differing substantially in directional plausibility.

The evidence is not uniform across all landscapes. NSGA-III remains marginally best on DTLZ1 with $M = 5$ and on DTLZ2 with $M = 5$ and $M = 10$, while CMOEA-CD obtains the best mean on DTLZ4 with $M = 5$. The WFG subset is also more balanced. The Friedman test does not reject comparable performance among the three algorithms on this subset ($\chi^2 = 2.000$, $p = 3.68 \times 10^{-1}$), and PBI-BFS-MaOA and NSGA-III have the same average rank, 1.833. This result is consistent with the fact that WFG includes disconnected, deceptive, degenerate, and highly multimodal structures, where different failure modes can dominate.

Even so, the WFG results support the specific role of active-niche filtering. PBI-BFS-MaOA obtains the best mean value on all three WFG1 instances and on WFG3 for $M = 8$ and $M = 10$. On WFG3 with $M = 10$, it obtains $\Delta_p = 7.23$, compared with 14.2 for NSGA-III and 15.2 for CMOEA-CD. On WFG3 with $M = 8$, the corresponding values are 2.60, 7.14, and 8.31. Since WFG3 is degenerate, these cases are aligned with the intended effect of active-niche filtering: when only a subset of directions is supported by the leading front, limiting insertion to active niches can prevent the algorithm from allocating survivors to weakly justified directions.

Runtime results support a balanced interpretation. Across instances, NSGA-III requires 10.69 s on average, PBI-BFS-MaOA requires 14.73 s, and CMOEA-CD requires 50.28 s. The proposed method is therefore approximately 37.8% slower than NSGA-III, but 70.7% faster than CMOEA-CD. Wilcoxon testing indicates that these runtime differences are systematic ($p < 1.2 \times 10^{-7}$ in each pairwise comparison). Across all 24 instances, the global Friedman test still favors PBI-BFS-MaOA, with average ranks of 1.625, 1.833, and 2.542 for PBI-BFS-MaOA, NSGA-III, and CMOEA-CD, respectively ($\chi^2 = 11.083$, $p = 3.92 \times 10^{-3}$).

Taken together, the results position PBI-BFS-MaOA as a quality–cost compromise. It is costlier than NSGA-III, substantially cheaper than CMOEA-CD, and frequently stronger in high-dimensional or degenerate settings where boundary-

ISSN:1390-9266 e-ISSN:1390-9134 LAJC 2026
DOI: https://doi.org/10.33333/lajc.vol13n2.04

TABLE I. Statistical results obtained by NSGA-III, CMOEA-CD, and PBI-BFS-MaOA on the DTLZ and WFG problems (Δ_p)

Problem	M	NSGA-III	CMOEA-CD	PBI-BFS-MaOA	Best	Gain (%)
DTLZ Suite						
DTLZ1	5	**6.63e-02 ± 2.8e-04**$^{=}$	2.73e-01 ± 3.9e-01^{-}	6.75e-02 ± 7.0e-04^{-}	NSGA-III	1.75
	8	2.00e-01 ± 1.7e-01^{-}	1.41e+00 ± 1.4e+00^{-}	**1.09e-01 ± 1.2e-03**$^{=}$	PBI-BFS-MaOA	45.19
	10	4.71e-01 ± 7.6e-01^{-}	4.44e+00 ± 3.7e+00^{-}	**1.46e-01 ± 1.2e-02**$^{=}$	PBI-BFS-MaOA	68.91
DTLZ2	5	**1.99e-01 ± 4.5e-05**$^{=}$	2.24e-01 ± 3.9e-03^{-}	1.99e-01 ± 4.7e-04^{-}	NSGA-III	0.17
	8	3.37e-01 ± 1.6e-04^{-}	4.92e-01 ± 2.0e-02^{-}	**3.35e-01 ± 7.4e-04**$^{=}$	PBI-BFS-MaOA	0.48
	10	**3.97e-01 ± 3.2e-04**$^{=}$	7.06e-01 ± 6.7e-02^{-}	4.03e-01 ± 1.8e-03^{-}	NSGA-III	1.32
DTLZ3	5	1.73e+00 ± 1.6e+00^{-}	1.52e+00 ± 1.5e+00^{-}	**3.79e-01 ± 5.4e-01**$^{=}$	PBI-BFS-MaOA	75.09
	8	1.43e+01 ± 7.3e+00^{-}	1.98e+01 ± 1.1e+01^{-}	**1.54e+00 ± 2.4e+00**$^{=}$	PBI-BFS-MaOA	89.21
	10	2.19e+01 ± 7.9e+00^{-}	7.56e+01 ± 6.6e+01^{-}	**1.52e+00 ± 1.5e+00**$^{=}$	PBI-BFS-MaOA	93.07
DTLZ4	5	2.42e-01 ± 1.1e-01$^{=}$	**2.17e-01 ± 3.8e-03**$^{=}$	2.61e-01 ± 1.2e-01$^{=}$	CMOEA-CD	16.80
	8	3.39e-01 ± 1.6e-02^{-}	4.51e-01 ± 9.7e-03^{-}	**3.36e-01 ± 8.2e-04**$^{=}$	PBI-BFS-MaOA	1.12
	10	4.07e-01 ± 2.3e-02$^{=}$	5.56e-01 ± 1.7e-02^{-}	**4.00e-01 ± 2.3e-03**$^{=}$	PBI-BFS-MaOA	1.78
WFG Suite						
WFG1	5	1.73e+00 ± 1.4e-02^{-}	1.94e+00 ± 1.4e-02^{-}	**1.69e+00 ± 1.8e-02**$^{=}$	PBI-BFS-MaOA	2.69
	8	2.47e+00 ± 6.3e-02^{-}	2.87e+00 ± 2.1e-02^{-}	**2.32e+00 ± 4.6e-02**$^{=}$	PBI-BFS-MaOA	6.01
	10	2.90e+00 ± 7.3e-02^{-}	3.36e+00 ± 4.0e-02^{-}	**2.65e+00 ± 7.7e-02**$^{=}$	PBI-BFS-MaOA	8.54
WFG2	5	**7.47e-01 ± 2.3e-01**$^{=}$	8.31e-01 ± 7.6e-02$^{=}$	8.64e-01 ± 2.9e-01$^{=}$	NSGA-III	13.56
	8	**1.93e+00 ± 6.5e-01**$^{=}$	2.24e+00 ± 9.6e-02^{-}	2.26e+00 ± 6.4e-01$^{=}$	NSGA-III	14.73
	10	**2.70e+00 ± 7.3e-01**$^{=}$	3.00e+00 ± 1.5e-01^{-}	2.73e+00 ± 8.3e-01$^{=}$	NSGA-III	1.09
WFG3	5	**1.67e+00 ± 2.4e-01**$^{=}$	2.67e+00 ± 3.8e-02^{-}	1.79e+00 ± 1.2e-01^{-}	NSGA-III	6.60
	8	7.14e+00 ± 8.5e-01^{-}	8.31e+00 ± 1.5e-01^{-}	**2.60e+00 ± 2.6e-01**$^{=}$	PBI-BFS-MaOA	63.53
	10	1.42e+01 ± 9.8e-01^{-}	1.52e+01 ± 1.8e-01^{-}	**7.23e+00 ± 5.4e-01**$^{=}$	PBI-BFS-MaOA	49.15
WFG4	5	1.72e+00 ± 8.7e-03^{-}	**1.50e+00 ± 3.9e-02**$^{=}$	1.74e+00 ± 6.8e-03^{-}	CMOEA-CD	13.65
	8	5.32e+00 ± 5.0e-02^{-}	**4.80e+00 ± 8.9e-02**$^{=}$	5.30e+00 ± 1.3e-02^{-}	CMOEA-CD	9.45
	10	7.73e+00 ± 1.2e-01^{-}	**7.46e+00 ± 1.1e-01**$^{=}$	7.54e+00 ± 3.2e-02^{-}	CMOEA-CD	1.14

front competition is prominent.

V. Conclusion and Future Work

This paper addressed many-objective optimization from a deliberately local standpoint. Instead of replacing the global Pareto scaffold, PBI-BFS-MaOA strengthens the decision made inside the final overflowing front. The method preserves Pareto ranking at the population level and introduces cumulative ideal–nadir normalization, PBI-based association, active-niche restriction, and occupancy-aware insertion only where standard survivor selection becomes least discriminative. Its contribution is therefore a boundary-front survival mechanism, not a new decomposition framework, a new generalized-dominance relation, or a multiarchive architecture.

The experimental evidence supports this design as a competitive alternative. Across the 24 benchmark instances, PBI-BFS-MaOA obtains the best overall Friedman rank and performs especially well on difficult DTLZ cases and on WFG3 as the number of objectives increases from 5 to 8 and 10. The strongest results occur in the more crowded configurations, where boundary-front competition is expected to be most severe. The WFG results are more mixed: NSGA-III remains strongest on WFG2, CMOEA-CD retains an advantage on WFG4, and the Friedman test on the WFG subset does not indicate a statistically significant separation among the three methods. Runtime places PBI-BFS-MaOA between the two baselines, so its practical value lies in a better quality–cost compromise than CMOEA-CD, although it does not match the lower computational cost of NSGA-III.

These findings suggest a practical recommendation for high-dimensional optimization tasks in engineering design, logistics, scheduling, resource allocation, and related decision systems: when a reference-guided algorithm repeatedly faces large boundary fronts, a localized PBI-based truncation rule can improve survivor quality without requiring a full redesign of the evolutionary framework. The method should not be read as a universal replacement for established reference-guided or archive-based approaches. It is better understood as a robust survival alternative for crowded or degenerate many-objective fronts.

Future work should follow three directions. First, a dedicated ablation study should separate the individual effects of dimensional scaling, active-niche filtering, and occupancy-aware insertion. Second, the feasibility branch defined through constraint violation should be evaluated on constrained DTLZ/WFG variants and engineering design benchmarks, since the present numerical study is limited to unconstrained problems. Third, sensitivity tests around the active-niche coverage threshold should be carried out to determine whether the conservative $0.8K$ gate remains appropriate across broader front geometries and population sizes.

Acknowledgment

The authors would like to thank METISBR: A Brazilian research group dedicated to Multi-Objective and Many-Objective Optimization (MaOPs) (https://github.com/METISBR), for the valuable discussions and the entire team's support during the development of this paper.

References

[1] B. Li, J. Li, K. Tang, and X. Yao, "Many-objective evolutionary algorithms: A survey," *ACM Computing Surveys*, vol. 48, no. 1, pp. 1–35, 2015.

[2] T. Santos and R. H. C. Takahashi, "On the performance degradation of dominance-based evolutionary algorithms in many-objective optimization," *IEEE Transactions on Evolutionary Computation*, vol. 22, no. 1, pp. 19–31, 2018.

[3] M. Pal, S. Saha, and S. Bandyopadhyay, "Decor: Differential evolution using clustering based objective reduction for many-objective optimization," *Information Sciences*, 2018.

[4] Q. Zhang and H. Li, "Moea/d: A multiobjective evolutionary algorithm based on decomposition," *IEEE Transactions on Evolutionary Computation*, vol. 11, no. 6, pp. 712–731, 2007.

ISSN:1390-9266 e-ISSN:1390-9134 LAJC 2026
DOI: https://doi.org/10.33333/lajc.vol13n2.04

[5] K. Li, K. Deb, Q. Zhang, and S. Kwong, "An evolutionary many-objective optimization algorithm based on dominance and decomposition," *IEEE Transactions on Evolutionary Computation*, vol. 19, no. 5, pp. 694–716, 2015.

[6] K. Deb and H. Jain, "An evolutionary many-objective optimization algorithm using reference-point-based nondominated sorting approach, part i: Solving problems with box constraints," *IEEE Transactions on Evolutionary Computation*, vol. 18, no. 4, pp. 577–601, 2014.

[7] Y. Yuan, H. Xu, B. Wang, and X. Yao, "A new dominance relation-based evolutionary algorithm for many-objective optimization," *IEEE Transactions on Evolutionary Computation*, vol. 20, no. 1, pp. 16–37, 2016.

[8] R. Cheng, Y. Jin, M. Olhofer, and B. Sendhoff, "A reference vector guided evolutionary algorithm for many-objective optimization," *IEEE Transactions on Evolutionary Computation*, vol. 20, no. 5, pp. 773–791, 2016.

[9] H. Ishibuchi, Y. Setoguchi, H. Masuda, and Y. Nojima, "Performance of decomposition-based many-objective algorithms strongly depends on pareto front shapes," *IEEE Transactions on Evolutionary Computation*, vol. 21, no. 2, pp. 169–190, 2017.

[10] W. Qiu, J. Zhu, G. Wu, M. Fan, and P. N. Suganthan, "Evolutionary many-objective algorithm based on fractional dominance relation and improved objective space decomposition strategy," *Swarm and Evolutionary Computation*, 2021.

[11] S. Liu, Q. Lin, K.-C. Wong, C. A. C. Coello, J. Li, Z. Ming, and J. Zhang, "A self-guided reference vector strategy for many-objective optimization," *IEEE Transactions on Cybernetics*, vol. 52, no. 2, pp. 1164–1178, 2022.

[12] W. Li, Y. Chen, Y. Dong, and Y. Huang, "A solution potential-based adaptation reference vector evolutionary algorithm for many-objective optimization," *Swarm and Evolutionary Computation*, vol. 85, p. 101451, 2024.

[13] S. Wang, H. Wang, Z. Wei, F. Wang, Q. Zhu, J. Zhao, and Z. Cui, "A pareto dominance relation based on reference vectors for evolutionary many-objective optimization," *Applied Soft Computing*, vol. 152, p. 111505, 2024.

[14] T. Santos and S. Xavier, "Pymoolab: An open-source visual analytics framework for multi-objective optimization using llm-based code generation and mcdm," 2026, preprint available at https://arxiv.org/abs/2603.01345.

[15] C. Zhu, L. Xu, and E. D. Goodman, "Generalization of pareto-optimality for many-objective evolutionary optimization," *IEEE Transactions on Evolutionary Computation*, vol. 20, no. 2, pp. 299–315, 2016.

[16] Y. Tian, R. Cheng, X. Zhang, Y. Su, and Y. Jin, "A strengthened dominance relation considering convergence and diversity for evolutionary many-objective optimization," *IEEE Transactions on Evolutionary Computation*, vol. 23, no. 2, pp. 331–345, 2019.

[17] S. Zhu, L. Xu, E. Goodman, K. Deb, and Z. Lu, "A general framework for enhancing relaxed pareto dominance methods in evolutionary many-objective optimization," *Memetic Computing*, vol. 14, pp. 289–308, 2022.

[18] S. Zhu, L. Zeng, and M. Cui, "Symmetrical generalized pareto dominance and adjusted reference vector cooperative evolutionary algorithm for many-objective optimization," *Symmetry*, vol. 16, no. 11, pp. 1–22, 2024.

[19] J. Cheng, G. G. Yen, and G. Zhang, "A many-objective evolutionary algorithm with enhanced mating and environmental selections," *IEEE Transactions on Evolutionary Computation*, vol. 19, no. 4, pp. 592–605, 2015.

[20] D. Sharma and P. K. Shukla, "Line-prioritized environmental selection and normalization scheme for many-objective optimization using reference-lines-based framework," *Swarm and Evolutionary Computation*, 2019.

[21] P. B. Myszkowski and M. Laszczyk, "Diversity based selection for many-objective evolutionary optimisation problems with constraints," *Information Sciences*, 2021.

[22] S. Liu, J. Zheng, Q. Lin, and K. C. Tan, "Evolutionary multi and many-objective optimization via clustering for environmental selection," *Information Sciences*, vol. 578, pp. 930–949, 2021.

[23] Z. Liu, F. Han, Q. Ling, H. Han, and J. Jiang, "Constraint-pareto dominance and diversity enhancement strategy-based evolutionary algorithm for solving constrained multiobjective optimization problems," *IEEE Transactions on Evolutionary Computation*, vol. 29, no. 6, pp. 2771–2784, 2025.

[24] K. Deb, L. Thiele, M. Laumanns, and E. Zitzler, "Scalable test problems for evolutionary multiobjective optimization," in *Evolutionary Multiobjective Optimization: Theoretical Advances and Applications*. London, U.K.: Springer, 2005, pp. 105–145.

[25] S. Huband, L. Barone, L. While, and P. Hingston, "A scalable multi-objective test problem toolkit," *Lecture Notes in Computer Science*, vol. 4193, pp. 280–295, 2006.

[26] O. Schütze, X. Esquivel, A. Lara, and C. A. C. Coello, "Using the averaged hausdorff distance as a performance measure in evolutionary multiobjective optimization," *IEEE Transactions on Evolutionary Computation*, vol. 16, no. 4, pp. 504–522, 2012.

ISSN:1390-9266 e-ISSN:1390-9134 LAJC 2026
DOI: https://doi.org/10.33333/lajc.vol13n2.04

AUTHORS

Thiago Santos

Thiago Santos is an Associate Professor at the Federal University of Ouro Preto (UFOP), Ouro Preto, Brazil. He holds a Ph.D. in Mathematics and coordinates both the Mathematics Education Research Group (GEEMA) and the Applied Mathematics Group of the Department of Mathematics. His research spans multi-objective optimization, evolutionary computation, and mathematics education, with special attention to the interaction between rigorous mathematical modeling and computational methods. In optimization and computational intelligence, his work focuses on the design and analysis of metaheuristic algorithms able to handle several conflicting objectives simultaneously, with applications in engineering and applied sciences. He also develops research in mathematics education, addressing pedagogical innovation, curriculum organization, and the conceptual barriers faced by students in advanced mathematical reasoning. Through this integrated agenda, he contributes to the theoretical foundations of optimization methods while supporting more effective approaches to university-level mathematics teaching. He is a founding member of the METISBR research group on multi-objective and many-objective optimization.

Sebastião Xavier

Sebastiao Xavier is an Associate Professor at the Federal University of Ouro Preto (UFOP), Brazil. He received his B.S., M.Sc., and Ph.D. in Mathematics from the Federal University of Minas Gerais (UFMG), developing specialized expertise in dynamical systems and real foliations. His academic career includes extensive teaching experience from basic education to graduate-level mathematics, together with sustained participation in the institutional development of mathematics programs at UFOP. Through the Mathematics Education Research Group (GEEMA), he has contributed to the training of future educators and to discussions on mathematical formation. His current scientific work is centered on optimization, especially multiobjective optimization and evolutionary strategies. In this area, he is interested in connecting rigorous theoretical foundations with computational procedures that can support practical decision-making. His research profile combines pure mathematics, applied optimization, educational engagement, and academic service. He is a member of the METISBR research group on multi-objective and many-objective optimization.

ISSN:1390-9266 e-ISSN:1390-9134 LAJC 2026